RSC Sustainability

ROYAL SOCIETY OF CHEMISTRY

PAPER

View Article Online
View Journal | View Issue

Cite this: *RSC Sustainability*, 2026, **4**, 1615

Biobased epoxy resins from itaconic anhydride functionalized lignin: insights and comparison with succinic analogues

Celeste Libretti,[ab] Gianluca Giuseppe Rizzo,[b] Sophia Abou El Mirate,[b] Mats Johansson *[cd] and Michael A. R. Meier *[ab]

Lignin, the most abundant renewable aromatic polymer, remains underutilized despite its potential as a sustainable feedstock for polymeric materials. In this work, lignin was functionalized with itaconic and succinic anhydrides to introduce carboxylic acid groups, enabling its use as a polyfunctional macromonomer. The influence of temperature, reaction time, reagent stoichiometry, and catalysts on the functionalization efficiency was systematically investigated. The resulting lignin derivatives were incorporated as crosslinkers into fully biobased epoxy resins formulated with epoxidized soybean oil and Pripol™ 1009, and their mechanical and thermal properties, as well as insights into the curing, were investigated in detail. Elastic moduli ranged from 4.87 to 1.24 MPa. The glass transition temperature (between −36 and −23 °C) was found to be primarily influenced by the aliphatic matrix, while the lignin content and the resulting network architecture strongly affected the mechanical properties of the materials. Comparative studies with succinic anhydride modified lignin highlighted the role of unsaturation due to itaconic acid in the network, especially for mechanical properties. Finally, degradation studies demonstrated depolymerization under alkaline hydrolysis, suggesting potential for designing easily cleavable thermoset systems. This work contributes to the development of greener epoxy networks and highlights lignin's versatility as a reactive renewable building block for sustainable polymer chemistry.

Received 25th January 2026
Accepted 7th February 2026

DOI: 10.1039/d6su00045b

rsc.li/rscsus

Sustainability spotlight

The growing need for renewable and degradable materials calls for alternatives to fossil-based thermosets, which are often non-recyclable and environmentally persistent. This work advances the sustainable valorization of lignin – a major but underutilized renewable resource – by developing an efficient and greener functionalization route with itaconic anhydride, a biobased reagent. The resulting lignin derivatives enable the preparation of fully biobased epoxy resins with tunable mechanical properties and chemical degradability under mild alkaline conditions. This approach contributes to a circular materials economy by reducing waste, improving resource efficiency, and utilizing renewable carbon sources. The work directly aligns with UN Sustainable Development Goals 9 (Industry, Innovation and Infrastructure), 12 (Responsible Consumption and Production), and 13 (Climate Action).

Introduction

Lignin is the most abundant source of aromatic compounds found in nature, and yet severely underutilized in nowadays materials. Lignin originates in nature from oxidative coupling of three monolignols, namely *p*–coumaryl alcohol, coniferyl alcohol, and sinapyl alcohol.[1] Interestingly, recent investigations have shown that other compounds, such as hydroxystilbenes or hydroxycinnamic amides, also contribute to the macromolecular structure of lignin, participating in the radical coupling reactions in several species.[2–4] This highlights the complexity of lignin's architecture and may be one of the reasons for lignin's underutilization, as it is typically burned for energy production.[5]

The majority of technical lignins is available *via* the kraft pulping process, with only a very small part of the global production used in applications for designing and producing materials with higher commercial and technological value. Lignin can be isolated from lignocellulosic biomass through various pulping processes, among which kraft pulping accounts for the majority of the annual lignin production. In addition to

[a]*Institute of Biological and Chemical Systems-Functional Molecular Systems (IBCS-FMS), Karlsruhe Institute of Technology (KIT), Kaiserstraße 12, Karlsruhe 76131, Germany. E-mail: m.a.r.meier@kit.edu; Web: www.meier-michael.com*

[b]*Institute of Organic Chemistry (IOC), Karlsruhe Institute of Technology (KIT), Kaiserstraße 12, Karlsruhe 76131, Germany*

[c]*Department of Fibre and Polymer Technology, Division of Coating Technology, KTH Royal Institute of Technology, SE-10044 Stockholm, Sweden. E-mail: matskg@kth.se*

[d]*Department of Fibre and Polymer Technology, Wallenberg Wood Science Center (WWSC), KTH Royal Institute of Technology, SE-10044 Stockholm, Sweden*

kraft pulping, organosolv pulping represents a widely established alternative with rapidly growing market demands.[6] It relies on the use of organic solvents, offering an environmentally friendlier method for lignin isolation, with potential for solvent recovery.[7] Furthermore, this process yields a sulfur-free lignin, typically characterized by lower molecular weights compared to kraft lignin.[8] Organosolv pulping was the isolation method for the lignin employed in this work.

Valorization of lignin has seen extensive research and advancements, typically to yield low-molecular weight products,[9] biocomposites, lignin-derived carbon fibers,[10] supercapacitors, bio-oil, and syngas, or to generate power.[11–13] However, lignin's structure and heterogeneity often hinder its application in polymer chemistry. The underutilization of this widely available and renewable material highlights the need for effective strategies to improve its upcycling and valorization. There is growing interest in using lignin in polymer synthesis to take advantage of its valuable properties; however, the sustainability and renewability of the underlying synthetic methods are frequently overlooked. Waste generation in combination with toxicity issues are in most cases still not addressed sufficiently, but these are important aspects of sustainability. Recently, we summarized the state of the art on lignin modification protocols, taking into consideration parameters such as the Environmental Factor (E-Factor), renewability and toxicity of the used reagents and their precursors.[14] Unfortunately, fossil-based as well as highly toxic functionalizing agents (most typical for lignin epichlorohydrin, ECH) are still widely employed – for instance to achieve epoxidized lignin, leaving significant room for further improvements.

Lignin offers a wide variety of functional groups, mainly hydroxyl (aliphatic and aromatic) and carboxylic acid groups, available for further modification. In particular, lignin can be used in the development of several resin types, offering a more sustainable alternative to petroleum-based products, such as in phenol-formaldehyde resins (PFs),[15,16] polyurethanes (PUs),[17,18] or non-isocyanate polyurethanes (NIPUs)[19–21] as well as epoxy resins.[22,23]

Among these materials, epoxy resins have attracted considerable attention, thanks to their excellent mechanical and thermal properties, broadening their range of application and expanding their global market.[24] However, inherent challenges associated with lignin epoxidation using ECH, as well as the reliance on petroleum-derived BADGE (bisphenol-A diglycidyl ether, a bisphenol-A derivative), and the toxicity concerns linked to fossil-based (as well as renewable)[25] amine hardeners, still remain.[26]

Lately, several renewable epoxy resin examples have been reported in the literature, based on renewable feedstocks such as plant oils[27,28] or cashew nut shell liquid (CNSL),[29] as well as biobased platform chemicals, such as levulinic acid, furfuryl amine,[30] syringaldehyde,[31] or vanillin.[32] However, even for these more sustainable alternatives, the introduction of epoxy groups still relied heavily on ECH chemistry, and despite the commercialization of glycerol-to-epychlorohydrin (GTE) plants, ECH still presents concerns related to its handling, toxicity and CMR rating.[33]

An additional sustainability challenge is related to the employment of typical amine hardeners presenting toxicity issues.[34,35] In this regard, other well-known crosslinkers for epoxy resins, namely anhydride[36] and carboxylic acid[37] curing agents, would be a less hazardous and potentially more sustainable approach. Interesting approaches for the introduction of carboxylic acid moieties onto lignin have recently been reported through carboxymethylation[38] or oxidative carboxylation with acetic acid and hydrogen peroxide.[39]

Several studies have reported the functionalization of lignin with cyclic anhydrides to obtain polycarboxylic acid–functionalized lignin, which can be directly employed as a crosslinker in various resin systems. For instance, Zhen *et al.*[40] reported fully bio-based epoxy resins from epoxidized soybean oil (ESBO) and tung oil anhydride-modified lignin, whereas Ma *et al.*[41] presented a multicarboxyl lignin hardener from glycidol and maleic anhydride, which was used to achieve bio-based epoxy resins, aided by citric acid and ESBO. Other examples involve modification of lignin with succinic acid,[42] succinic anhydride,[43–45] as well as maleic anhydride to achieve thermosets *via* thiol- and amine-based Michael additions.[46]

Epoxidation of unsaturated vegetable oils is commonly achieved through peracid-mediated reactions (often generated *in situ*) *via* chemical or chemo-enzymatic routes.[47] ESBO was selected as renewable epoxy crosslinker to furthermore address the toxicity concerns associated with conventional ECH-based epoxy resins, as outlined above. ESBO-based epoxies are known to exhibit lower mechanical performance than conventional fossil-based glycidyl ether–based systems (*e.g.*, BADGE). Within this framework, lignin is introduced as a rigid, multifunctional macromolecular component to partially compensate for the intrinsic flexibility of ESBO.

To the best of our knowledge, lignin modification with itaconic anhydride (IAn) has not yet been reported in the literature. IAn, compared to the structurally related maleic anhydride, is renewable (maleic anhydride production still relies on *n*-butane)[48] and less harmful.[49–51] IAn is derived from the dehydration of itaconic acid, a well-known bio-based platform chemical produced *via* fermentation, and was first reported in 1837 by thermal decomposition of citric acid.[52,53] This study presents detailed investigations of the functionalization reaction of lignin with itaconic anhydride. Reaction conditions were thoroughly optimized and the resulting itaconate-functionalized lignin carefully characterized. IAn was then employed for the synthesis of fully renewable epoxy resins, in combination with ESBO and Pripol™ 1009, a dimeric diacid with a monocyclic core unit, obtained from the Diels–Alder reaction of unsaturated long chain fatty acids.[54,55]

Lignin was likewise functionalized with succinic anhydride under the same reaction conditions. The resulting derivatives were subsequently employed in analogous experiments to obtain epoxy resins, allowing a direct comparison of the two anhydride-modified lignins in epoxy resin applications.

Results and discussion

Lignin functionalization with itaconic anhydride and subsequent characterization

The functionalization of lignin with itaconic anhydride was optimized by systematically varying the reaction conditions such as temperature, reaction time, and reagent stoichiometry, in an initial 0.5 g reaction scale. The progress and outcome of the functionalization were monitored by ^{31}P-NMR and IR spectroscopy, as well as size exclusion chromatography (SEC). Typically, the extent of esterification is associated with an increased amount of carboxylic acid (–COOH) and ester (COOR) groups, as illustrated in Scheme 1. Moreover, an increase in molecular weight is expected.

At the initial stage, the reaction was conducted under bulk conditions in an effort to minimize solvent use and align with the principles of green chemistry. However, these conditions proved impractical, as achieving a homogeneous mixture between the molten anhydride and lignin required a very large excess of IAn. Even with a large excess (10 equiv.), a proper dispersion of lignin could not be achieved, as the mixture remained inhomogeneous. The use of a reaction solvent—despite introducing an additional component—was considered more practical, especially if the solvent could be easily recovered by distillation. For this reason, organosolv lignin (OL) was fractionated in acetone prior to the functionalization step and characterized in detail (see SI, Table S2). Acetone was chosen as the reaction solvent for its ability to solubilize all the components and being easily recoverable. Additionally, acetone does not raise major concerns from a health and environmental impact point of view, as depicted by the GSK's solvent selection guide.[56] Moreover, solvent recovery was also included in our work, as will be discussed later.

The performance of four different base catalysts was investigated. Organic superbases are known to catalyze transesterification reactions,[57,58] and therefore three different superbases, namely 1,8-diazabicyclo[5.4.0]undec-7-ene (DBU), 1,5,7-triazabicyclo[4.4.0]dec-5-ene (TBD), and 1,1,3,3-tetramethylguanidine (TMG) were tested, as well as the heterogeneous inorganic base potassium carbonate (K_2CO_3). DBU and TMG showed comparable performance, with DBU showing slightly higher catalytic activity (0.96 mmol g^{-1} of –COOH installed, *vs.* 0.92 mmol g^{-1} of –COOH with TMG as the catalyst), as shown in Table 1, entries 1–4 and Fig. 1. TBD and K_2CO_3 were less active. In addition to the environmental impact, it is important to compare the two catalysts in terms of toxicity (DBU: acute toxicity cat. 3, $LD50_{oral,\ rat}$ = 215–681 mg kg^{-1}, TMG: acute toxicity cat. 4 $LD50_{oral,\ rat}$ = 835 mg kg^{-1}).[59,60] Thus, TMG can be categorized as less toxic than DBU. The experimental data further show similar conversions of TMG and DBU (50% and 54% conversion of aliphatic hydroxyl groups for TMG and DBU, respectively). To ensure consistency and direct comparability across the optimization study, DBU was retained as the primary catalyst using a fixed set of reaction conditions (1.4 IAn equiv., 45 °C, 24 h and 6 $_{mol}$% cat. loading), while individual parameters were systematically varied, despite the lower toxicity of TMG. Nevertheless, the reaction was subsequently upscaled with both catalysts, confirming that TMG performs comparably and demonstrating that the reaction proceeds efficiently in either case (SI, page S9–S10).

Different catalyst amounts were also tested and compared to uncatalyzed conditions. Initially, under the same reaction conditions, the addition of 6, 12, and 100 mol% of DBU was investigated (Table 1, entries 5–7). A catalyst amount of 6 mol% was beneficial to obtain functionalization with IAn; however, increasing the amount of catalyst to above 6 mol% led to a rather high amount of insoluble fraction formation during the reaction, probably due to side reactions (*i.e.,* crosslinking *via* Oxa-Michael addition or salt formation between the excess superbase and the newly formed –COOH groups) that prevented a reliable investigation on the extent of the reaction. For 12 mol% of DBU, only the soluble fraction could be analyzed, while for 100 mol% DBU the reaction mixture turned completely insoluble after a few minutes, as already observed in the work from Olsén *et al.*[61] in their functionalization of lignin with maleic anhydride with 4-dimethylaminopyridine (DMAP) as the catalyst. In contrast, the reaction performed in the absence of a catalyst exhibited minimal conversion, as indicated by IR spectroscopy results (Fig. S7, SI), highlighting the essential function of the latter.

Following functionalization, all samples exhibited higher M_n values relative to the starting material (OL acetone (1); M_n: 2900,

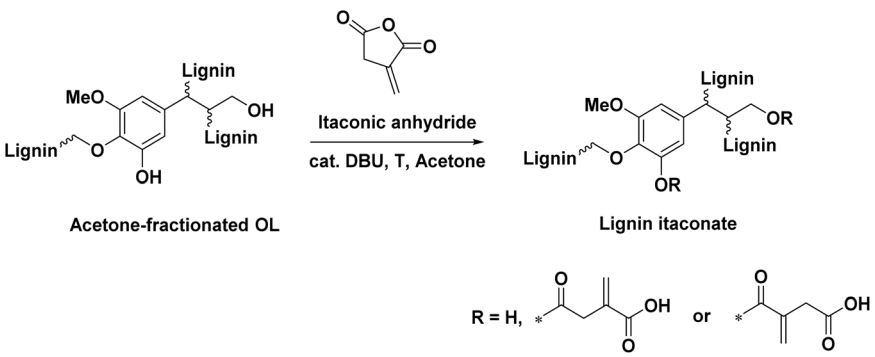

Scheme 1 General reaction scheme of the functionalization of lignin with itaconic anhydride; representative structures of lignin and lignin itaconate are shown.

Table 1 Effect of different parameters on the reaction between lignin and itaconic anhydride. Conditions: 0.5 g of dried, acetone fractionated lignin (OL acetone 1) was dissolved in 5 ml of dry acetone. The vessel was flushed with argon and heated to the desired temperature. Equivalents of the functionalizing agent, catalyst, catalyst amount and time were tested. r.t.: room temperature[a,b]

Entry	IAn (equiv.)	T (°C)	Cat.	Cat. (mol%)	Time (h)	Aliphatic (mmol g^{-1})/ ($X_{Aliphatic}$, %)[c]	Aromatic (mmol g^{-1})/ ($X_{Aromatic}$, %)[c]	–COOH (mmol g^{-1})[c]	Mn (Da)[d]	Đ[d]
Catalyst influence										
1	1.4	45	**DBU**	6	24	1.01 (54)	1.76 (23)	0.96	3800	16
2	1.4	45	**TBD**	6	24	1.34 (41)	1.56 (30)	0.73	3700	4.9
3	1.4	45	**K2CO3**	6	24	1.26 (44)	1.62 (28)	0.78	3800	4.9
4	1.4	45	**TMG**	6	24	1.11 (50)	1.53 (31)	0.92	4200	8.1
Catalyst amount										
5	1.4	45	**DBU**	6	24	1.01 (54)	1.76 (23)	0.96	3800	16
6a	1.4	45	**DBU**	12	24	0.93 (57)	1.59 (29)	0.97	3800	6.4
7b	1.4	45	**DBU**	100	24	Insoluble fraction formation				
Time										
8	1.4	45	**DBU**	6	3	1.45 (37)	1.62 (28)	0.69	3500	3.8
9	1.4	45	**DBU**	6	16	1.32 (41)	1.91 (17)	0.88	4100	9.2
10	1.4	45	**DBU**	6	24	1.01 (54)	1.76 (23)	0.96	3800	16
Temperature										
11	2.1	r.t.	**DBU**	6	16	1.21 (46)	1.40 (36)	0.92	3700	4.1
12	2.1	45	**DBU**	6	16	0.69 (67)	1.37 (38)	1.07	4000	20
13[a]	2.1	66	**DBU**	6	16	0.5 (76)	1.18 (45)	1.27	5600	15
IAn equivalents										
14	0.7	45	**DBU**	6	16	1.60 (31)	2.28 (5)	0.51	3200	4.1
15	1.4	45	**DBU**	6	16	1.32 (41)	1.91 (17)	0.88	4100	9.2
16	2.1	45	**DBU**	6	16	0.69 (67)	1.37 (38)	1.07	4000	20
17	4.2	45	**DBU**	6	16	0.66 (69)	1.17 (46)	1.45	4000	5.9

[a] Partial formation of the insoluble fraction. Only the soluble fraction was analyzed. [b] Complete insoluble fraction formation; no analysis possible. [c] Data calculated from ^{31}P-NMR. Conversion (%) is standardized for the increase in molecular weight of the educt compared to the starting material (see the SI for calculations). [d] SEC solvent is dimethylacetamide-lithium bromide (DMAc-LiBr) (0.034%).

M_w: 7800, $Đ$: 2.7) as well as an increase in dispersity. These observations are consistent with the findings of Olsén *et al.*,[61] where the increased dispersity after functionalization was mitigated by fractionation. In our case, however, this step was deliberately omitted to avoid additional solvent usage. The effect of functionalization on molecular weight and thermal properties depends on the nature of the introduced moieties: the addition of the more rigid itaconate groups increases molecular weight and restricts chain mobility, as demonstrated by the higher T_g values (140 °C) compared to those of the starting material acetone-fractionated lignin (T_g = 125 °C).

Increasing the reaction time was found to be beneficial for a higher extent of functionalization. Reaction times of 3, 16, and 24 h were investigated as time intervals for the transesterification reaction. While longer reaction times consistently led to higher –COOH contents, the increase in mmol g^{-1} of functionalities between 16 h (0.88 mmol –COOH per g) and 24 h (0.96 mmol –COOH per g) indicated that further extension yielded only marginal benefit. In addition, excessively long reaction times are less attractive from a process efficiency perspective. Thus, 24 h was selected as an upper practical limit (Table 1, entries 8–10).

The influence of the reaction temperature was investigated at r.t., 45 °C and 66 °C, respectively (Table 1, entries 11–13). The results indicate an increase in the carboxylic acid group functionalities with increasing temperature. Nonetheless, the reaction conducted at 66 °C led to a high amount of insoluble solid fraction formation that prevented an accurate quantification of the outcome of the reaction. Moreover, these conditions (10 °C above the boiling point of acetone) would render the scaling up of the reaction more impractical. Therefore, 45 °C was chosen as the optimal temperature. By varying the equivalents of IAn from 0.7 to 4.2, the amount of installed –COOH groups in the esterified lignin and the molecular weight increased considerably (Table 1, entries 14–17), as confirmed by IR spectroscopy (Fig. 1). Signals associated with successful conversion can be ascribed to the increasing C=O stretching vibrations of both the ester (1764 cm^{-1}, forming between the lignin backbone and anhydride) and the free carboxilic acid (1730 cm^{-1}). Additionally, the intensity of the emerging signal at 1649 cm^{-1}, attributed to the C=C stretching vibration of the Michael system, increased with an increasing degree of functionalization.

As general trends, longer reaction times and higher equivalents of IAn were found to enhance the overall reaction

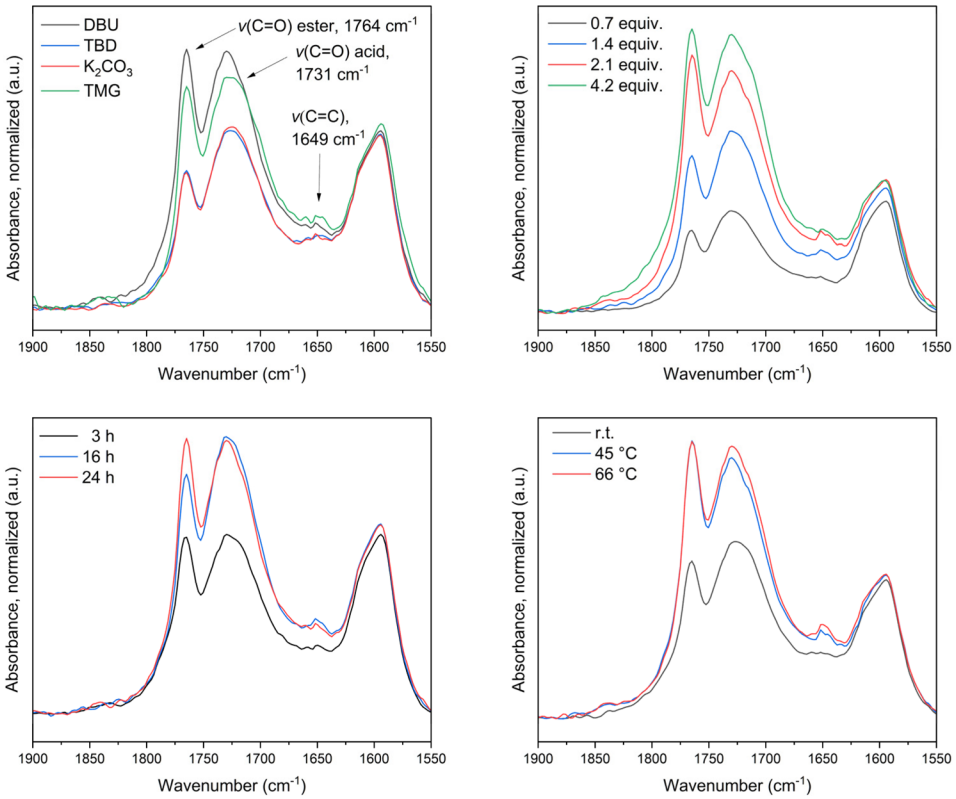

Fig. 1 Overlay of the IR spectroscopy reaction monitoring in the region of 1900–1550 cm^{-1} with different parameters tested. All IR spectra are normalized to the signal at 1504 cm^{-1} for the lignin $C_{ar} = C_{ar}$ stretching vibrations.

conversion. Increased temperatures promoted higher reactivity with the drawback of promoting the occurrence of side reactions, indicated by solidification. Therefore, 45 °C was identified as a compromise between conversion and selectivity. Across all samples, the aliphatic hydroxyl groups displayed higher reactivity than the phenolic –OH groups, with a maximum conversion of 46% observed for the aromatic –OH groups, as indicated by ^{31}P-NMR results.

Literature reports show that the exo-double bond of IAn can undergo isomerization to the thermodynamically more stable citraconic anhydride (CIAn).[62,63] In order to investigate the stability of the double bond in the IAn structure, different screenings were carried out in the absence of lignin. Initially, IAn and DBU were mixed in acetone and heated to 45 °C to replicate the reaction conditions, and aliquots were taken over time and analyzed *via* NMR spectroscopy. Corresponding data suggest that the isomerization of the double bond takes place almost immediately, reaching close to complete isomerization of the double bond after 10 minutes (Fig. S8, SI). This is in accordance with literature findings, where the isomerization is favored in the presence of tertiary amines.[59] For comparison, K_2CO_3 and TMG were also tested and exhibited comparable isomerization results to DBU (Fig. S8, SI). These findings suggest that IAn predominantly isomerizes during the reaction and CIAn is most likely the functionalizing agent reacting with lignin, as depicted in Scheme 2. Therefore, while the products

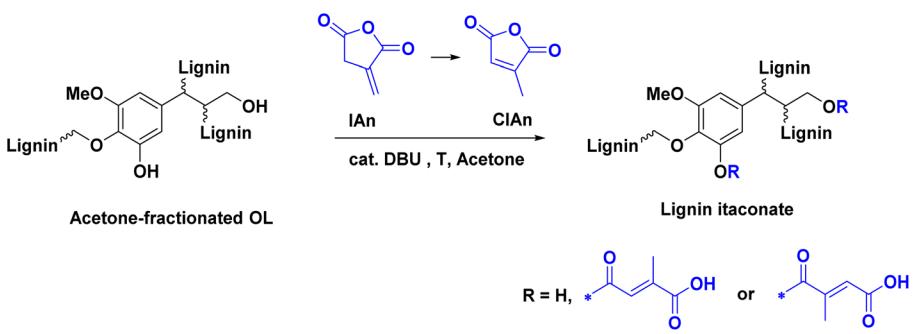

Scheme 2 General reaction scheme of isomerized itaconic anhydride (CIAn) and a representative structure of lignin.

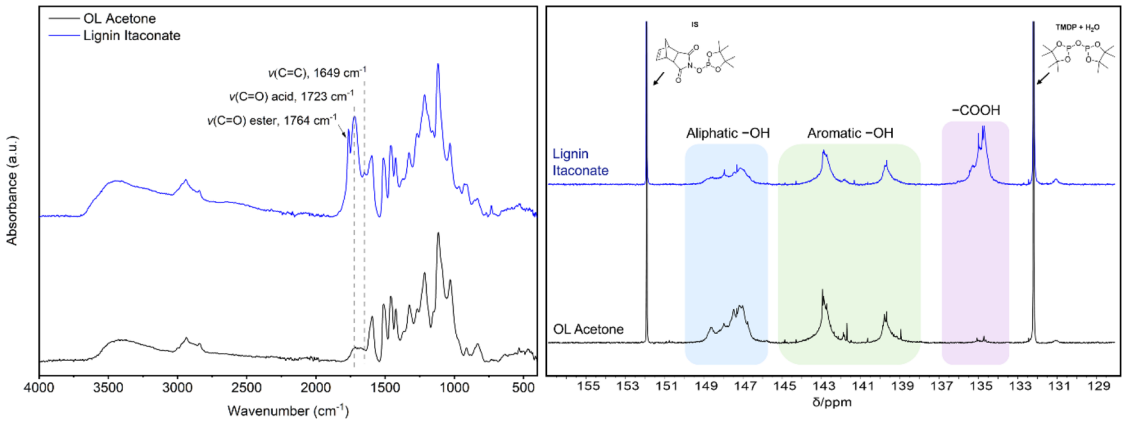

Fig. 2 Left: representative IR spectra of acetone-fractionated OL (OL Acetone, starting material) and LI. Right: ^{31}P-NMR spectra highlighting the change in the characteristic signals for aliphatic hydroxyl (light blue), aromatic hydroxyl (green) and carboxylic acid groups (purple).

are referred to as Lignin Itaconates (LIs) throughout this work for consistency, the structure likely corresponds predominantly to lignin citraconates. Despite this isomerization, carboxylic acid groups remain incorporated into the modified lignin structure, facilitating the resulting macromonomer to be applied in thermoset systems that rely on –COOH reactivity. Furthermore, the introduced Michael system is still retained, although its reactivity may be reduced compared to the non-isomerized case, as the literature postulates.[64,65]

To enable the use of LI in thermoset applications, a larger-scale synthesis (15 g) was conducted with optimized reaction conditions. A complete characterization of the product, also for the TMG-catalyzed upscaled reaction, can be found in the SI, demonstrating that the scale-up effectively works with both catalysts (DBU and TMG).

Fig. 2 presents the IR spectrum of the upscaled reaction product, confirming the successful functionalization through the characteristic signals associated with the insertion of the citraconate moieties. The corresponding ^{31}P-NMR spectrum further supports this assumption, indicating a pronounced increase in the –COOH region relative to the starting material. In particular, the upscaling conditions led to a –COOH value of (1.39 ± 0.02) mmol g^{-1}.

From HSQC analysis (Fig. 3) of both the fractionated lignin in acetone (OL Acetone) and the LI, structural understandings can be obtained. Signals ascribed to pinoresinol (structure **B**) remain unchanged after modification. A shift in the signals of structures such as β-O-4' (**A**) and phenylcoumaran (**C**) from δ_C/δ_H 61–65/3.5–3.9 ppm to δ_C/δ_H 62–65/4–4.44 ppm can be observed after modification of the primary hydroxyl groups. To the best of our knowledge, it was not possible to precisely differentiate between the signals of A_γ and C_γ. Nevertheless, a shift of the signals is clearly visible, confirming the successful functionalization. However, the signal ascribed to A_α did not

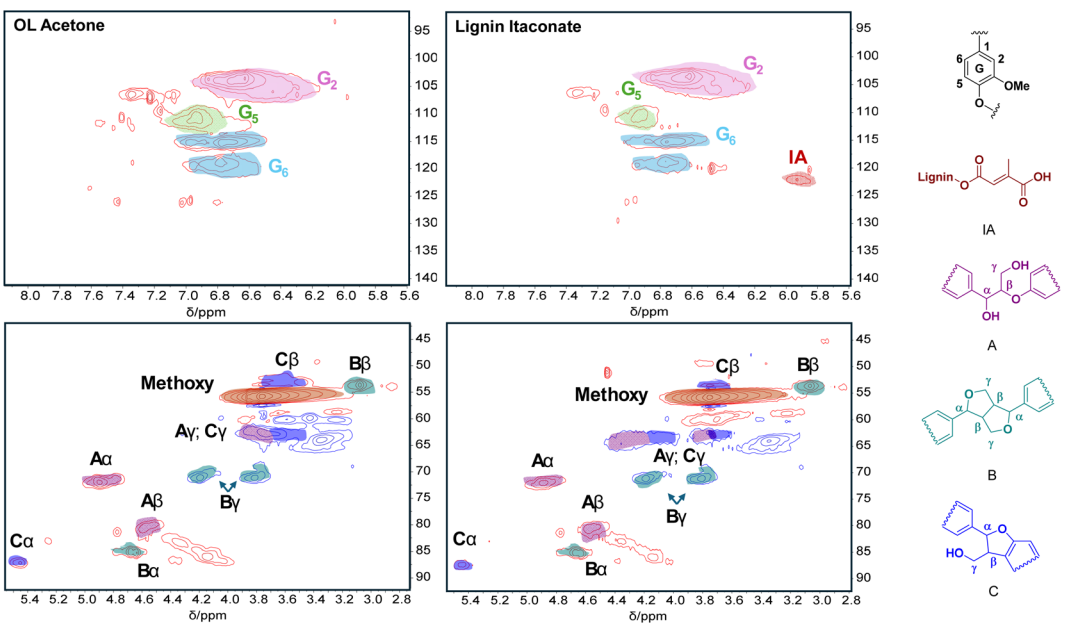

Fig. 3 HSQC traces of acetone fractionated lignin (OL acetone (2)) and itaconic functionalized lignin.

shift, showing that the reactivity of the modification was not very high with secondary hydroxyl groups (as also demonstrated *via* ^{31}P-NMR, aliphatic –OH are still present after modification, with (0.90 ± 0.004) mmol g^{-1}). In the aromatic region, a new signal appears (IA, δ_C/δ_H 122/5.92 ppm), ascribed to the proton of the double bond of the IA moiety (isomerized, indicated as the IA structure in Fig. 3). Complete HSQC analysis is available in the SI (Fig. S6).

Environmental factor, recyclability of the solvent, and the precipitation medium

As highlighted recently, the modification of lignin with cyclic anhydrides remains one of the most promising pathways for developing low environmental-factor (E-factor) protocols to access carboxylic acid functionalized lignin.[14] Indeed, the waste streams generated are typically associated with catalysts, solvents, and excess reactants. In this context, bulk conditions and a minimal amount of catalyst would be beneficial to lower the overall E-factor of the procedure. As mentioned above, bulk conditions were not feasible with IAn, due to the high excess of reactant required to achieve adequate mixing with lignin. In order to enhance the overall sustainability of the functionalization process, efforts were thus directed towards solvent recovery (Table 2). Due to the large volume of water required for precipitation during workup, the distillation proved challenging, ultimately leading to a recovery rate of 75% of the initially used acetone (characterization of the recovered solvent is provided in the SI (Fig. S9)). As a proof of concept, the recovered acetone was dried over molecular sieves for 72 h and subsequently employed in a new functionalization reaction. However, the conversion of the aliphatic groups was lower in comparison to that when using fresh anhydrous acetone, likely due to residual water presence.

The precipitation medium used for the esterification reaction with the recovered acetone was reused multiple times for additional reactions, demonstrating its reusability. During the experiments, denoted as reutilization of the precipitation medium (LI-RPM#), the differences in the conversion were monitored *via* IR spectroscopy. Prior to each reuse, the medium was filtered to remove any residual solids. LI-RPM1 and LI-RPM2 exhibited an almost identical spectrum, while a slight decrease begins with LI-RPM3, followed by a more noticeable decline in LI-RPM4 (Fig. S10, SI). These results suggest that the precipitation medium can be reused effectively at least three times without compromising precipitation efficiency, thereby contributing positively to the sustainability of the process.

Synthetic *E*-factor values were estimated using a simplified approach to highlight solvent impact on the total amount of waste, without considering the fractionation pretreatment and the workup. A detailed discussion of the calculation assumptions and limitations is provided in the SI. By implementing a simple recycling procedure of the solvent *via* distillation, it was possible to lower the total E-factor for the procedure from 6.9 to 2.7. In previous work,[14] several lignin modification strategies were reported, together with a comparative discussion of their E-factors. On comparing the E-factor of the lignin modification with itaconic anhydride described herein to conventional ECH-based routes, the present approach results in substantially lower values (typically between 4 and 16 for ECH-based systems).[14] Even alternative ECH-free routes reported in the literature, such as those involving epoxidation of fatty acid mixtures followed by esterification with lignin, were associated with considerably higher E-factors (E-factor: 38 for the overall sequence).[66] Also the esterification of organosolv lignin with oleyl chloride followed by epoxidation of the unsaturated bonds using peracetic acid resulted in a relatively high E-factor (E-factor: 14.2 for the entire sequence).[67]

Epoxy resin formulation

The optimal conditions established for the scale-up of lignin functionalization with itaconic anhydride were subsequently applied to its modification with succinic anhydride (SAn). SAn was selected as a saturated and unbranched analogue of IAn, allowing a direct comparison of reactivity and final material properties. This yielded a lignin succinate derivative (LS) with a –COOH content of 1.79 mmol g^{-1} (a complete characterization of this product is provided in the SI, Table S5).

With both LI and LS synthesized and characterized, their performance in the development of fully biobased epoxy resin systems was investigated. Initial efforts were dedicated to finding the optimal formulation for the thermosets, consisting of LI or LS as the lignin component, Pripol™ 1009 as the diluent and ESBO (rpoxidized soybean oil) as the epoxy component. A representative scheme of the reaction is shown in Scheme 3. The stoichiometric ratio of COOH : epoxy was chosen to be 1 : 1.2, which was previously reported to deliver the best performance in terms of mechanical properties and crosslinking density.[68–71] Different mol% of the lignin component were tested, namely 5, 10, 15, 25 and 35 mol% (with respect to the total amount of –COOH groups; the rest to achieve the desired functional group equivalents was covered by Pripol™; for detailed calculations see Table S6, SI). Due to the presence of

Table 2 Data comparison of the –OH group distribution in the modification of lignin with IAn utilizing fresh solvent (entry 1) and recovered solvent (entry 2). Conditions: 0.50 g of dry OL acetone and 1.40 equiv. of IAn (based on the lignin –OH value) were dissolved in dry acetone. DBU (6 mol%) was added, and the reaction mixture was stirred at 45 °C for 24 h

Entry	Total (mmol g^{-1})^a	Aliphatic (mmol g^{-1})^a	Aromatic (mmol g^{-1})^a	–COOH (mmol g^{-1})^a	$X_{Aliphatic}$ (%)^b	$X_{Aromatic}$ (%)^b
1-Fresh acetone	3.71	1.01	1.76	0.96	54	23
2-Recovered acetone	3.52	1.44	1.48	0.56	31	23

^{a} Determined from ^{31}P-NMR. ^{b} Conversion (%) is standardized for the increase in molecular weight of the product compared to the starting material (see the SI for calculations).

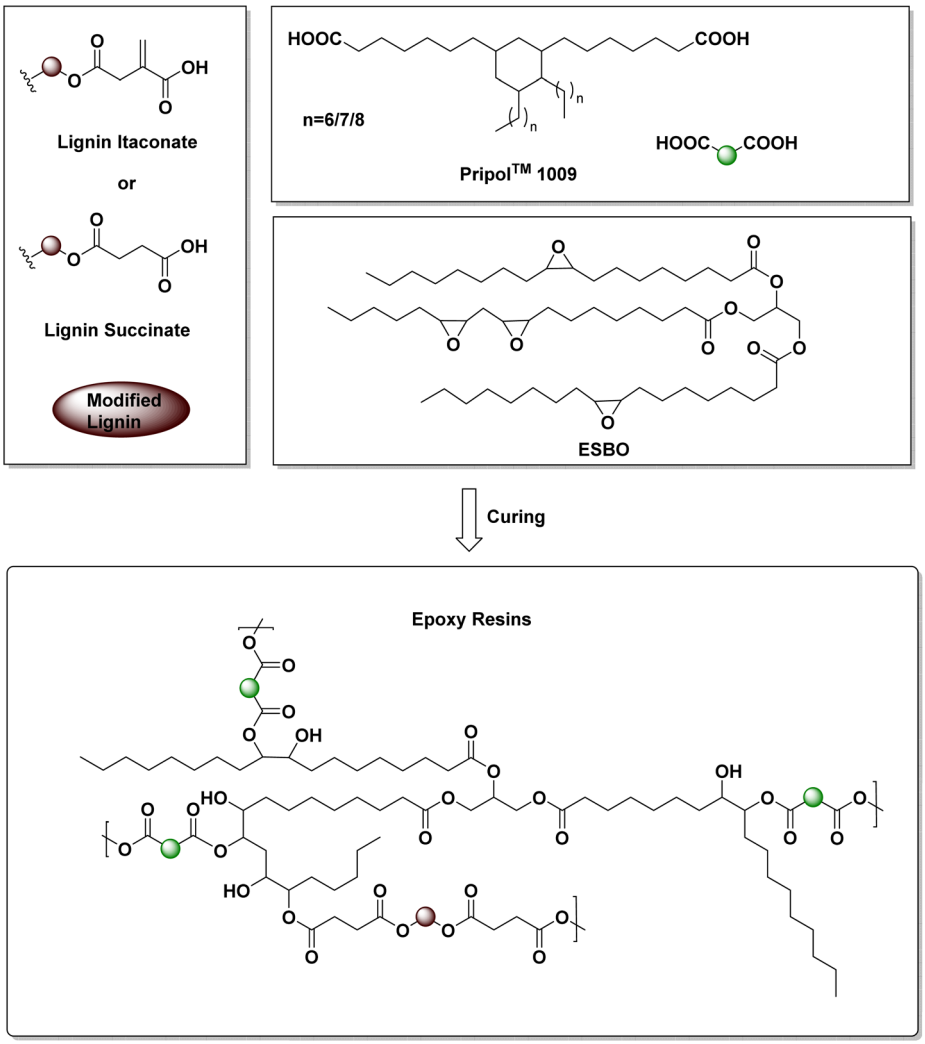

Scheme 3 General reaction scheme of the epoxy resin formation. The starting materials (lignin types LI or LS, Pripol™, and ESBO) as well as the final resins are shown with representative structures. LI is chosen as the default representative structure, but the isomerized structure (citraconate) is likely also present, as depicted in Scheme 2.

lignin, the resin mixtures required the use of a solvent to dissolve all the components prior to curing. Initially, acetone was selected as the solvent for resin preparation due to its ease of removal and ability to fully dissolve the carboxylic acid-functionalized lignin. However, in preliminary tests, phase separation was observed in the final materials for lignin contents above 5 mol% (Fig. S11, SI). This issue, likely ascribed to the rapid evaporation of acetone during processing, was effectively resolved by replacing acetone with dimethylsulfoxide (DMSO). To confirm that the high-boiling solvent DMSO is not present anymore in the final material after curing, possibly affecting the gel content or the mechanical properties of the material, the sample was weighed before and after curing. The total mass of the components without solvent was investigated before and after curing (m_i and m_f, respectively). The difference between the two values was $\Delta m = -10$ mg, showing no mass increase due to solvent left inside the material. The small difference in mass is within the error range of the measurement ($m_i = 344$ mg), probably due to small material losses while transferring the sample.

In Fig. 4, exemplary IR spectra of the resins are shown, along with a reference spectrum of ESBO. After curing, notable spectral changes can be observed: the characteristic stretching band of the oxirane ring, clearly visible in the ESBO spectrum, is not observed in either resin spectra, indicating that the epoxy groups have successfully reacted. In addition, an increase in the broad O–H stretching region is evident (3600–3100 cm^{-1}), consistent with the formation of β-hydroxy ester groups resulting from the epoxy-acid curing reaction. Additionally, the carbonyl stretching vibration of the resins displays a small shoulder at 1710 cm^{-1}, which may correspond to unreacted carboxylic acid groups.

A small amount of DBU (0.5 wt% with respect to the total resin mass) was necessary as the catalyst in order to achieve faster crosslinking. The IR spectra of the resins without and with 0.5 wt% of DBU as the catalyst are shown in Fig. S12 (SI). If

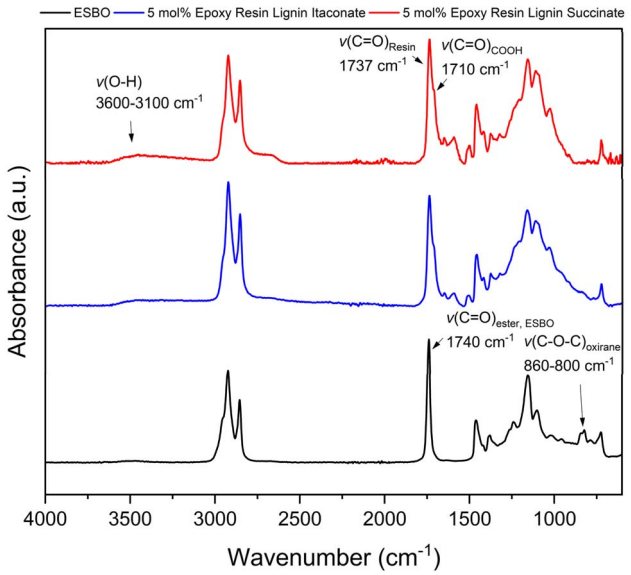

Fig. 4 Stacked IR spectra of ESBO (black curve), the epoxy resin with 5 mol% of lignin itaconate (blue curve), and epoxy resin with 5 mol% of lignin succinate (red curve).

the catalyst was not present in the formulation, the cured resins presented a splitting in the carbonyl region, where the signal at ~1750 cm^{-1} is ascribed to the carbonyl stretching vibration for the ester groups of ESBO, while the other peak (~1710 cm^{-1}) is attributed instead to the carbonyl stretching vibration of free unreacted –COOH. From the spectra presented in Fig. S12 (SI), it can be observed that under the same curing conditions, the reaction in the presence of the catalyst proceeded significantly faster.

Real-time IR spectroscopy was employed to monitor the curing of the resins over time. Two formulations containing 5 mol% of LI were analyzed, with and without DBU, as shown in Fig. 5. As a comparison, the curing behavior of the resin containing 5 mol% of LS was also monitored and is reported in Fig. S15 (SI). A closer inspection of the carbonyl region reveals that the shoulder peak at ~1700 cm^{-1}, attributed to free –COOH groups, decreases progressively in both systems, indicating ongoing esterification. In the presence of DBU as the catalyst, this shoulder becomes significantly less prominent within the observed time of ~3000 s, suggesting a more complete consumption of carboxylic acid groups. Simultaneously, a clear decrease in the intensity of the epoxy absorption band is observed, particularly in the catalyzed formulation, confirming an accelerated reaction rate.

To assess the evolution of the absorbance peak area associated with free –COOH groups over time, a peak deconvolution analysis was performed on the carbonyl region. The area of the signal compared to its initial value is plotted over time as shown in Fig. 6. A comparison was made to evaluate the catalyst

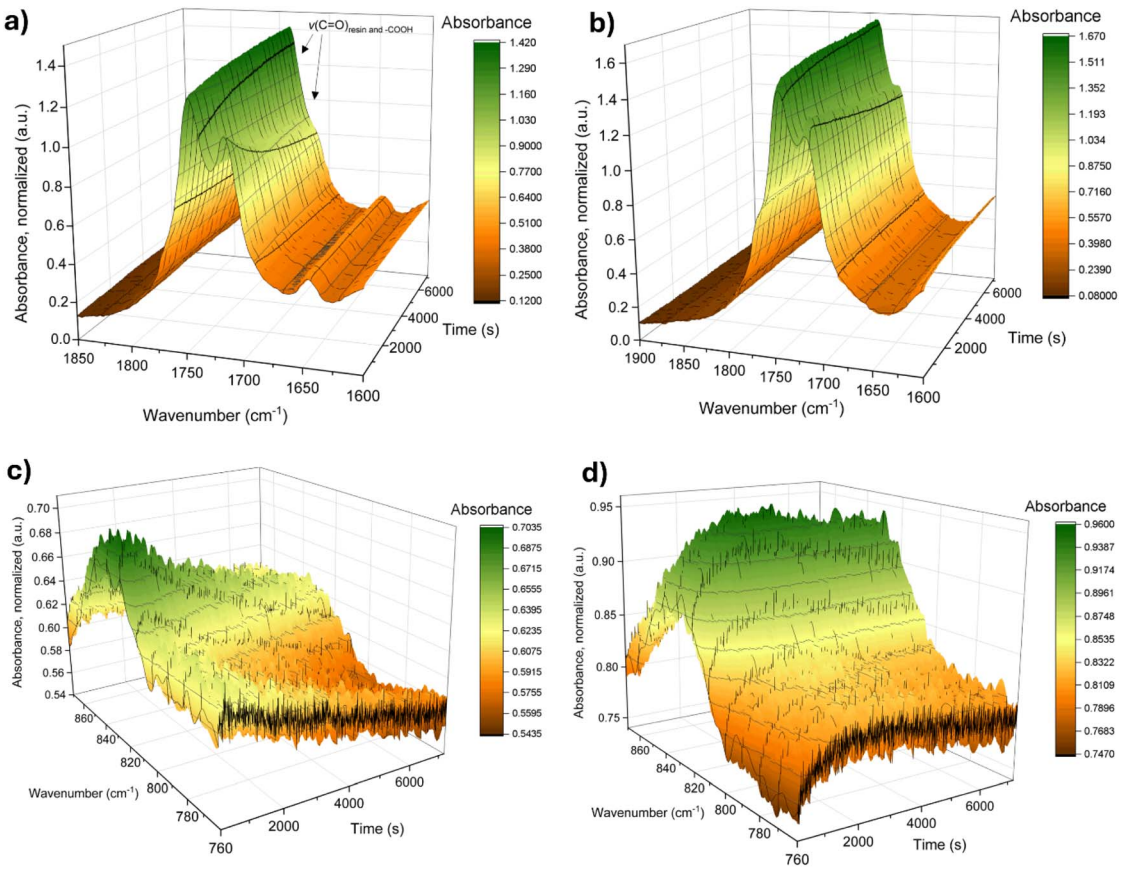

Fig. 5 Realtime IR curves of the 5 mol% lignin formulations, with (a and c) and without DBU (b and d). For both cases, a zoom-ed in view in the region of the carbonyl area (a and b, 1600–1850 cm^{-1}) and the epoxy region (c and d, 760–860 cm^{-1}) is presented over time.

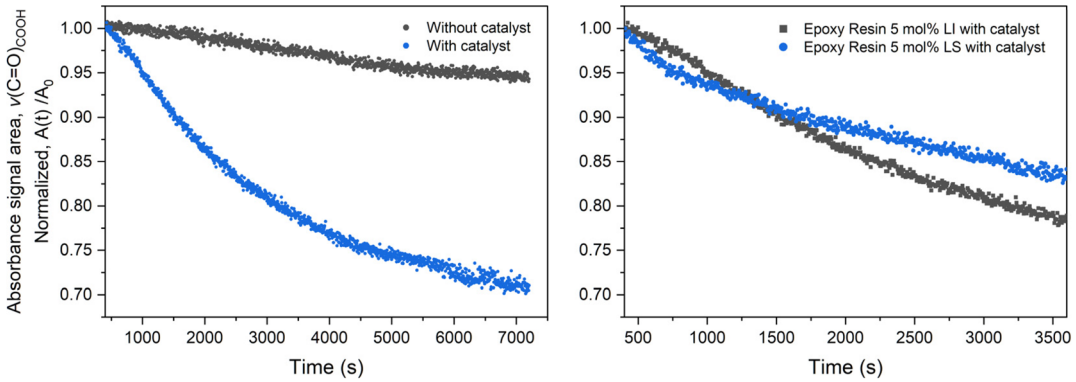

Fig. 6 Normalized absorbance signal area of the free –COOH groups over time. Left: an epoxy resin formulation with 5 mol% LI, with and without catalytic amounts of DBU. Right: two epoxy resin formulations with 5 mol% of LI or LS, both in the presence of catalytic amounts of DBU. The time range differs between the graphs (7000 s for LI and 3500 s for LS) due to practical instrument time constraints.

presence (Fig. 6, left) and the lignin type (Fig. 6, right). Details of the deconvolution procedure are provided on Page S18 (SI).

As depicted in Fig. 6, left, the normalized absorbance signal area for –COOH groups decreases much faster in the presence of DBU as the catalyst, confirming that its presence is necessary for a faster and efficient curing procedure. On the right, the normalized absorbance signal area corresponding to the –COOH groups is plotted over time for the resins containing 5 mol% of LI or LS, both cured under identical conditions and in the presence of DBU. Since the initial comparison on the left indicated that the curing reaction rate significantly decreased after approximately 4000 s, the acquisition time for the comparative experiment between the two lignin derivatives was limited to 3500 s, which was sufficient to evaluate potential differences in the curing kinetics between the two systems. The results suggest that the curing behavior of resin with LI proceeds slightly faster than the one with LS. However, considering the small lignin content in both resins (5 mol%), the overall curing kinetics are likely dominated by the Pripol™ matrix. Moreover, the final extent of –COOH consumption is similar for both systems, indicating comparable overall reactivity.

Different stoichiometric ratios were tested, and from their respective IR spectra it was possible to compare the relative amounts of free carboxylic acid compared to the ester carbonyl groups through a peak deconvolution method. The results show that with an excess of epoxy groups, more free carboxylic acids are converted and crosslinked within the network. In particular, going from a 1 : 1 to 1 : 1.5 COOH : epoxy ratio decreased the free fatty acid percentage ratio from 33 to 24% (SI, Fig. S14 and Table S7).

Table 3 Gel contents of the epoxy resins developed with varying contents of different lignin macromonomers LI and LS

Lignin content (mol%)	GC lignin itaconate (%)	GC lignin succinate (%)
0	78	78
5	84	90
10	83	90
15	81	85
25	81	92
35	83	91

The same range of lignin mol% compositions and optimized conditions (Table S6, SI) established for the LI-based resins were extended to the LS formulations. The gel contents (GCs) of 78–92% for all thermosets (see Table 3) confirm a successful network formation within the resins for both lignin macromonomers. The gel contents for LS are slightly higher than the ones for the resins obtained with LI, which can be attributed to higher –COOH functionalities of LS (1.79 mmol g^{-1} –COOH) compared to LI (1.39 mmol g^{-1} –COOH), thus increasing the crosslinking density. The relatively low GC values of the resins could be influenced by several factors. First, the internal epoxy groups of ESBO are intrinsically less reactive than terminal epoxy groups of established monomers such as DGEBA, showing lower crosslinking densities compared to other compounds bearing terminal epoxies.[72] Moreover, the structure of Pripol™, with its long aliphatic chain and bulky structure, could likely lead to reduced crosslinking density and lower reactivity compared to smaller, more rigid carboxylic crosslinkers such as linear aliphatic diacids, owing to steric effects, as also discussed in the work of Matharu *et al.*[73] In line with this, additional experiments were designed using shorter difunctional renewable acids (azelaic, C_9 and adipic, C_6) for resins containing 30 mol% of LI under identical curing conditions. The aim was to investigate the influence of Pripol™ on the GC, compared to shorter chain diacids. This indeed resulted in higher gel contents (92 and 95%, for azelaic and adipic, respectively) compared to the Pripol-based system (86%), but simultaneously resulted in very poor mechanical properties (the materials were glassy and very brittle), which rendered their handling and further analysis particularly challenging. Finally, Pripol™ provided a suitable compromise between successful network formation and favorable mechanical properties, slightly reducing the gel content, but still maintaining satisfactory values.

Thermal properties of the epoxy resins

Thermal analyses of the thermosets were performed using Differential Scanning Calorimetry (DSC) and Thermal

Table 4 Overview of the thermal data for the set of epoxy resins with LI and LS, as well as the starting lignin derivatives

Mol% lignin	T_g (°C)	$T_{d,5\%}$ (°C)	$T_{d,50\%}$ (°C)	Residues (%)	Lignin content (wt%)
0	−36	347	427	1	—
5–LI	−32	348	429	4	6
10–LI	−33	345	432	5	12
15–LI	−32	331	434	12	18
25–LI	−33	290	428	22	28
35–LI	−31	282	436	27	36
5–LS	−29	323	417	5	5
10–LS	−30	321	416	7	10
15–LS	−32	305	417	8	14
25–LS	−24	310	415	9	23
35–LS	−23	294	414	15	31
LI	140	213	441	36	—
LS	104	230	423	35	—

Gravimetric Analysis (TGA) measurements. All formulations exhibited relatively low glass transition temperatures (T_g) around −30 °C, consistent with the high flexibility observed at room temperature (DSC curves are reported in Fig. S16, SI). No clear correlation between lignin content and T_g values was identified for either functionalized lignin, suggesting that the highly aliphatic nature of the polymer matrix predominantly governs the thermal behavior. However, a slight increase in T_g was observed for higher lignin contents in the LS-based epoxy resins, indicating that the more rigid lignin structure may contribute to a modest restriction of chain mobility and thus a higher T_g.

The TGA curves (Fig. S17, SI) show that all the thermosets present increased thermal stability compared to the starting materials of modified lignin, which present lower $T_{d,5\%}$ (213 and 230 °C, for LI and LS, respectively) compared to the thermosets (with the lowest $T_{d,5\%}$ of 282 °C) (Table 4). The materials present single-step degradation curves, with the $T_{d,5\%}$ values decreasing with increased lignin content (from 347 °C for 0 mol% lignin to 282 and 294 °C for 35 mol% of LI and LS, respectively). This is likely due to the lower thermal stability brought by the starting lignin macromonomers. Residues are increasing as well with lignin content, which was expected because lignin contributes to char formation. The lower residues for the LS-type resins can be explained by a lower wt% of the lignin in the final materials, as the LS presented higher functionalization. An overview of the data is presented in Table 4.

Rheology and DMA experiments

Amplitude sweep and frequency sweep tests on the formulations containing 0, 5 and 10 mol% of LI (higher lignin contents were too brittle to be characterized mechanically) were conducted. The amplitude sweep tests were carried out to identify the linear viscoelastic region (LVER) and the behavior of the material within the LVER. All formulations presented a dominant elastic component with the storage modulus G′ > G″, and a clear solid-like behavior, as depicted in Fig. 7. Increasing the lignin content influences the LVER, making the materials more resistant to deformation and increasing the shear strain that can be applied to the materials before they start to undergo irreversible changes in their structure. This indicates that the incorporation of lignin itaconate into the thermoset matrix reinforces the network, likely due to the rigid, multifunctional nature of lignin, increasing crosslink density and restricting chain mobility. In the thermoset with the highest lignin content tested (10 mol%) the LVER ended at 13%, *versus* a 1.2% shear strain for the thermoset without lignin, suggesting that the presence of lignin itaconate in the thermoset matrix strongly contributes to the viscoelastic behavior of the materials. A frequency sweep (SI, Fig. S18) between 0.01 and 10 Hz also revealed a dominant storage modulus and a viscoelastic solid behavior in all the materials, confirming the results of the amplitude sweep.

Dynamic Mechanical Analysis (DMA) experiments were performed on the formulations with the lowest lignin contents to gain insights into the mechanical behavior of the materials. Specifically, resins containing 0 mol%, 5 mol% and 10 mol% of LI or LS were investigated. Fig. 8a presents the overlaid DMA curves. For each formulation, three to five replicates were analyzed to ensure reproducibility. All samples exhibited a sharp decrease in storage modulus (E′, Table 5) at the glass transition temperature (T_g, or T_α, corresponding to the α-relaxation). This pronounced drop, particularly near the instrument transducer's sensitivity limit, can introduce

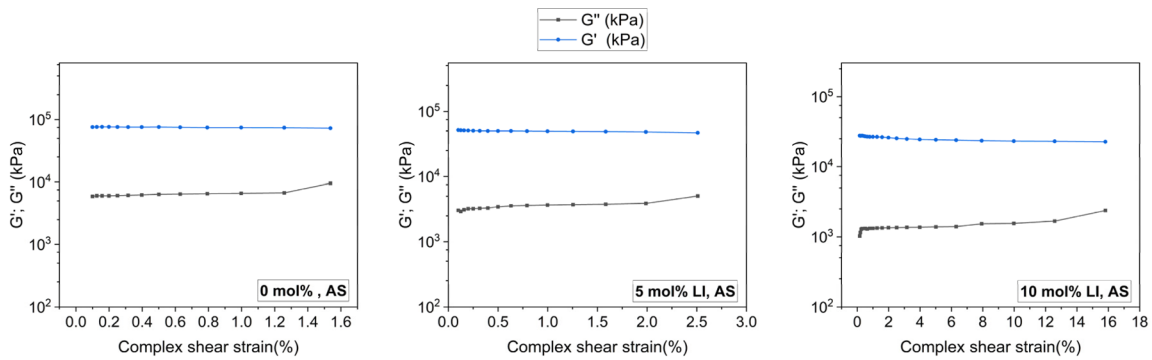

Fig. 7 Amplitude sweep experiments for LI epoxy resins with lignin contents of 0, 5, and 10 mol%.

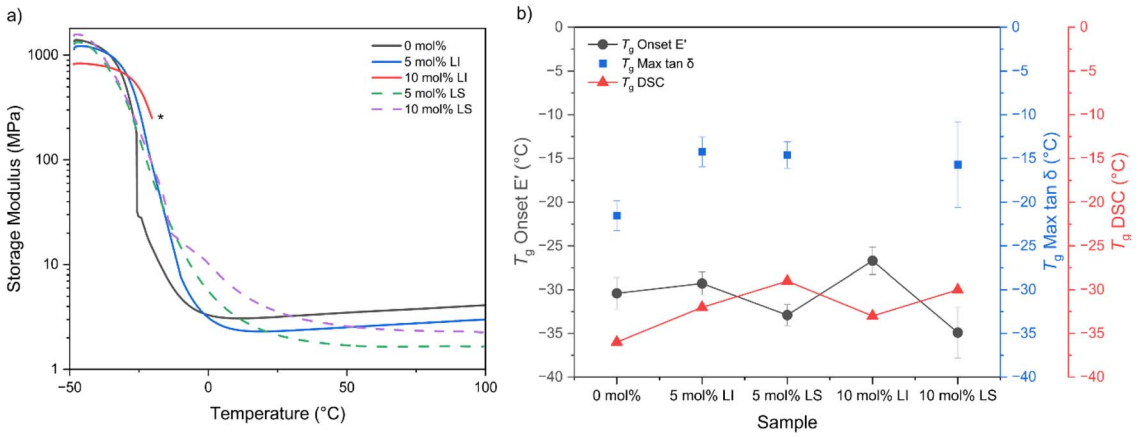

Fig. 8 (a) Representative DMA curves for the formulation tested. *: n.a. due to experimental difficulties (see SI, Fig. S19). (b) Comparison of the T_g values obtained from DMA and DSC methods.

Table 5 Overview of the most significant data obtained from DMA and tensile strength measurements

Sample	$E'_{-50°C}$ (MPa)	$E'_{25°C}$ (MPa)	$E'_{100°C}$ (MPa)	T_g (°C) onset E′	T_g (°C) max tan δ	Crosslinking density (x10^3 mol m^{-3})	Elastic modulus (MPa)	Ultimate stress (MPa)	Strain (%)
0 mol%	1242 ± 110	2.78 ± 0.38	3.47 ± 0.57	−30.4 ± 1.8	−21.54 ± 1.70	0.501 ± 0.12	1.97 ± 0.28	0.24 ± 0.06	13.1 ± 3.2
5 mol% LI	1352 ± 192	3.52 ± 1.04	4.42 ± 1.23	−29.28 ± 1.31	−14.25 ± 1.68	0.76 ± 0.34	2.78 ± 0.37	0.48 ± 0.06	17.2 ± 3.3
5 mol% LS	1138 ± 212	2.12 ± 0.004	1.68 ± 0.04	−32.9 ± 1.2	−14.6 ± 1.5	0.572 ± 0.03	1.24 ± 0.02	0.23 ± 0.02	20.9 ± 1.7
10 mol% LI	850 ± 85	—[a]	—[a]	−26.70 ± 1.57	—[a]	—[a]	4.87 ± 1.27	0.26 ± 0.06	6.5 ± 2.6
10 mol% LS	1311 ± 202	3.42 ± 0.17	2.15 ± 0.10	−34.9 ± 2.9	−15.7 ± 4.9	1.128 ± 0.04	1.83 ± 0.18	0.45 ± 0.03	26.0 ± 1.2

[a] n.a. Due to experimental difficulties (see SI Fig. S19).

experimental challenges, as reflected in some of the curve resolutions. In particular, the thermoset containing 10 mol% LI approached the detector limit, making data above the onset unreliable for quantitative interpretation. Despite these limitations, the thermosets displayed comparable maximum storage moduli in the glassy and rubbery regions, suggesting similar crosslinking densities. In particular, the crosslinking densities were calculated according to the theory of rubber elasticity (eqn. S5, SI). The results show a general trend of increasing crosslink density with higher lignin content, as expected from the incorporation of the polyfunctional macromonomer. This finding highlights how lignin incorporation can be used to tailor the network architecture and, consequently, the mechanical and viscoelastic properties of the thermosets. The relatively large standard deviations observed in some cases can be attributed to the intrinsic heterogeneity of the networks and the structural irregularities of the lignin derivatives. This can be regarded as a future challenge in lignin chemistry, as such deviations limit real world applications. As the materials transit through the glass transition region, their elasticity changes, leading to a minimum in the storage modulus. Fig. 8b shows that the T_g values determined by DMA (from the onset of E′) correlated well with those obtained by DSC. The T_g values derived from the maximum tanδ—higher than the onset ones—provide an indication of the glass transition region relevant for potential application conditions.

Tensile strength measurements of the resins

The investigation of mechanical properties provided further understanding of the behavior of the thermosets. Fig. 9a shows representative stress–strain curves for the different formulations. Thermosets prepared with LI exhibited higher elastic moduli compared to the other formulations, suggesting that the incorporation of itaconate moieties contributes to increased rigidity and stiffness, as can be expected in comparison to succinic moieties. These formulations also showed lower strain at break, indicating a more brittle behavior with a higher likelihood of structural defects. Conversely, thermosets prepared with LS displayed lower elastic moduli—even compared to the 0 mol% formulation—along with higher elongation at break, consistent with the introduction of more flexible succinate moieties into the network. In contrast to the thermal analysis results, the mechanical performance appears to be strongly influenced by both the lignin content and its chemical nature, indicating that the type and amount of lignin play a major role in defining the overall mechanical response of the otherwise aliphatic matrix. In Fig. 9b, an overview of the important parameters obtained from the stress–strain curves is presented. Table 5 summarizes the key results obtained from the DMA and tensile strength measurements. Once again, the large standard deviations observed in some cases confirm the heterogeneous nature of the materials, particularly for the formulation

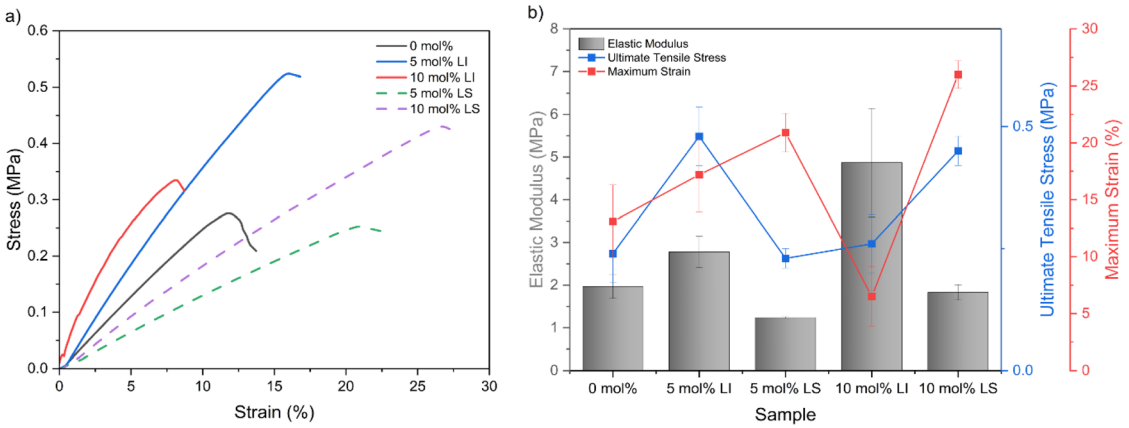

Fig. 9 (a) Representative stress–strain curves of the tested formulations. (b) Overview of the most significant parameters (elastic modulus, ultimate tensile stress and maximum strain) obtained from stress–strain curves of the formulations. For all the samples, 3 to 5 replicates were tested for each measurement.

containing 10 mol% LI. For this sample, five replicates were tested to ensure reproducibility. Such variability is typical for systems with high lignin contents.[74,75]

Degradation of the resins

Due to the presence of hydrolyzable ester bonds in the structure of the thermosets, we investigated if the materials could be degraded *via* hydrolysis. These include esters formed between the lignin backbone and the itaconate moieties, as well as esters resulting from the reaction of carboxylic acid groups (both from LI and Pripol™) with the epoxy groups of ESBO and the ester groups of ESBO itself. The degradation behavior was exemplarily studied on a 10 mol% LI epoxy resin. Both alkaline and acidic conditions were tested for the hydrolysis of the resin. A determined amount of 10 mol% LI epoxy resin was submerged in either an alkaline or acidic solution and stirred for 4 days at 80 °C. The outcome of the degradation was analyzed *via* IR spectroscopy and ^{31}P-NMR.

Acidic conditions were investigated, as in principle they represent a more sustainable option; in contrast to alkaline hydrolysis, they do not require a subsequent neutralization step to recover the product, which generates additional waste. Under acidic conditions in fact, the lignin fraction is expected to precipitate following the breakdown of the thermoset matrix. Two different acidic media were tested: a 1 M HCl solution and a 1 M citric acid (CA) solution, alongside a 0.6 M NaOH solution for the alkaline conditions, adapted from literature conditions.[46] The degradation conditions were kept identical for all treatments (4 days, 80 °C, for detailed experimental procedures see the SI). In both acidic cases, a brown, powdery precipitate was obtained after the reaction (see SI, Fig. S24b). This

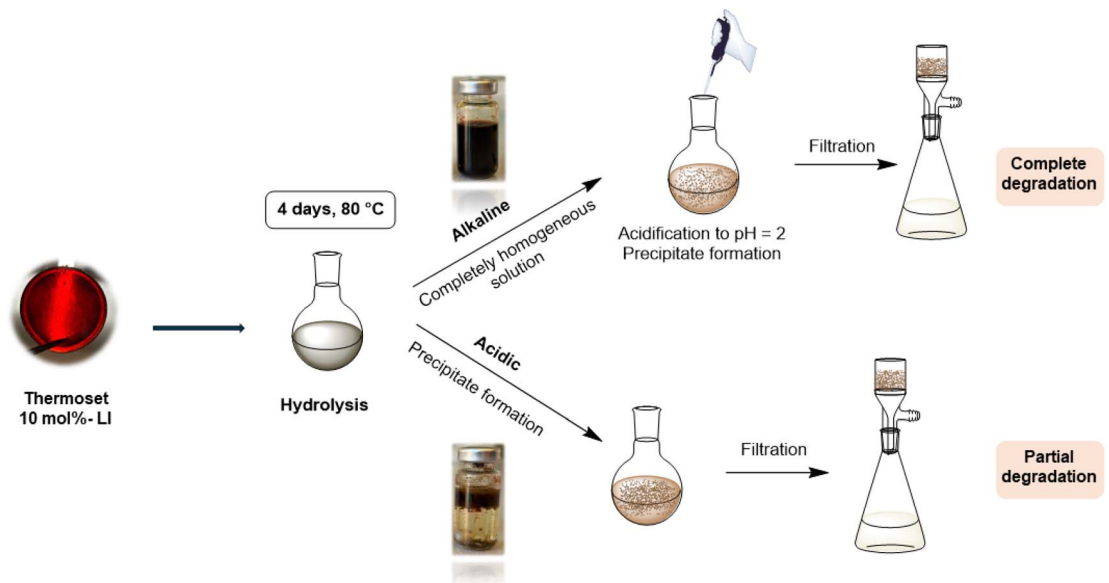

Scheme 4 Illustrative scheme for the degradation procedure of thermoset 10 mol% – LI under alkaline or acidic conditions.

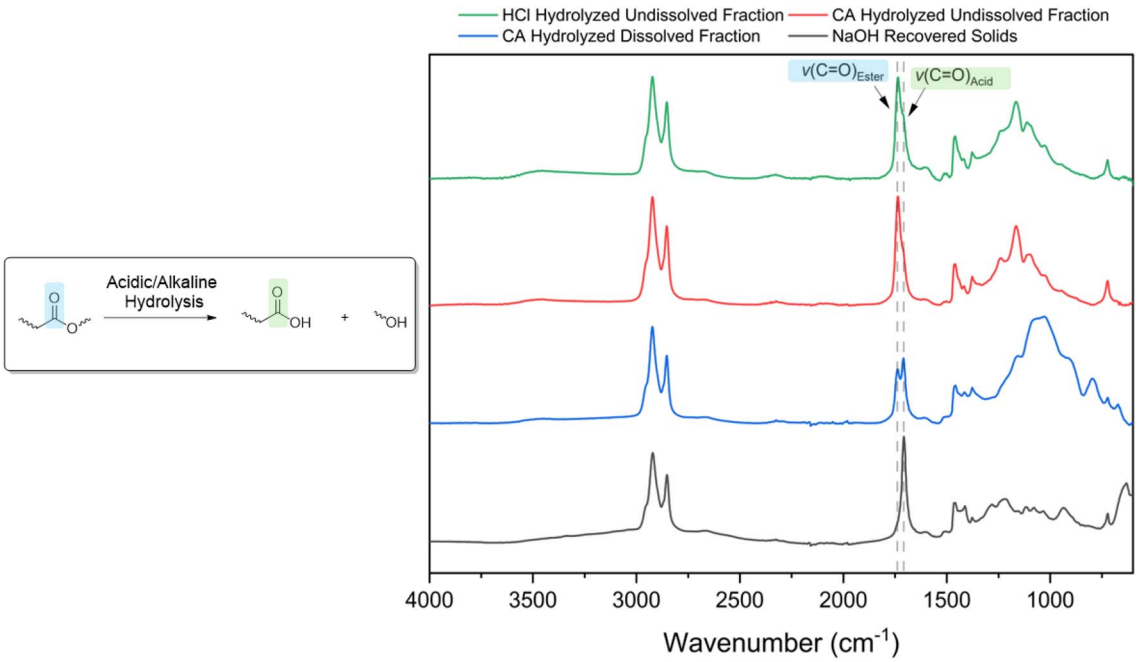

Fig. 10 IR spectrum overlay of the different collected hydrolysis fractions. The IR spectrum of the solids collected after alkaline hydrolysis (black spectrum) shows a complete disappearance of the stretching vibration signals for the ester carbonyl, sign that the degradation proceeded successfully. After acidic hydrolysis with citric acid (blue spectrum) there is a splitting in the carbonyl region, a sign that the degradation progressed only partially. The IR spectra of the undissolved fractions after acidic hydrolysis (red and green) are similar to those of the initial thermosets, a sign that the degradation was minimal.

precipitate was filtered, collected, and dried. Only partially degraded resin fragments were visually detected, even after four days of reaction, indicating that degradation under acidic hydrolysis proceeded only partially (Fig. S24c, SI). For clarity, in Scheme 4 the degradation procedures are illustrated.

To separate the remaining undegraded material, the solids were suspended in acetone, and the insoluble resin fragments were removed by hot filtration. This procedure yielded two distinct fractions: an undissolved portion corresponding to the remaining thermoset pieces, and a dissolved portion, which was subsequently recovered by precipitation in acidic water. For the sake of comparability between methods, the product from alkaline hydrolysis was also subjected to dissolution in acetone and reprecipitation; however, in this case, complete dissolution in the solvent was observed, indicating a successful and complete breakdown of the resin matrix. An overview of all collected fractions is provided in Table S8. Nevertheless, degradation under alkaline conditions proved highly effective, as confirmed by IR spectroscopy (Fig. 10, in black), which showed the complete disappearance of the ester carbonyl stretching band, leaving only the characteristic carbonyl signal of the carboxylic acid group stretching. The IR spectrum of the dissolved fraction obtained from citric acid hydrolysis (Fig. 10, in blue) still displayed characteristic ester carbonyl stretching vibration signals, indicating that the degradation process was incomplete.

The ^{31}P-NMR spectra of the recovered fractions (SI, Fig. S25) revealed a strong presence of aliphatic and carboxylic acid (–COOH) groups, with minimal to no signals corresponding to aromatic hydroxyl groups typically associated with lignin. These results confirm that probably only a limited amount of lignin was recovered in these fractions; however it is necessary to consider that the lignin content within the sample was low compared to the fatty acid content. In fact, even additional purification steps *via* dissolution and reprecipitation were not successful to isolate it, and the lignin fraction could not be recovered.

Overall, an efficient hydrolysis pathway for the resins was established, leading to complete degradation under alkaline conditions, but only partial degradation under acidic ones. These findings highlight the potential of such thermosetting materials for applications where controlled degradability under hot alkaline conditions is desirable, such as in packaging adhesives or removable labels. The combination of high bio-based content, flexibility and alkaline-hydrolyzable ester linkages suggests potential in applications where high stiffness is not required, but removability, elasticity and end-of-life degradability are advantageous.

Conclusions

In this work, a novel route for lignin functionalization with itaconic anhydride was developed and optimized. The influence of key reaction parameters – anhydride equivalents, catalyst, temperature, and reaction time – was systematically investigated. Under the applied conditions, isomerization of itaconic to citraconic anhydride occurred, consistent with literature reports, without affecting the introduced functional groups.

The process was successfully scaled up, yielding comparable conversion and product characteristics. The precipitation medium could be reused up to three times, and a solvent recovery of 75% reduced the synthetic E-factor from 6.9 to 2.7. The resulting lignin derivatives were incorporated as multifunctional crosslinkers in fully biobased epoxy resins alongside epoxidized soybean oil and Pripol™ 1009 and subsequently compared to analogous lignin succinate derivatives.

The thermosets exhibited high gel contents, thermal stability up to 280 °C, and low glass transition temperatures (ranging from −36 to −23 °C), consistent with their flexible and ductile behavior. Notably, resins based on lignin itaconate showed higher elastic moduli and lower strains at break, indicating enhanced stiffness from itaconate incorporation. Finally, degradation studies demonstrated complete hydrolysis under alkaline conditions and partial degradation in acidic media, highlighting the potential of these materials as cleavable, biobased epoxy networks for sustainable applications.

Conflicts of interest

There are no conflicts to declare.

Data availability

The data supporting this article have been included as part of the supplementary information (SI), including, but not limited to, instrument specifications and methods, complete characterization of the lignin samples, and additional analytical data for the epoxy thermosets, such as DSC and TGA traces, rheology, and DMA analyses. See DOI: https://doi.org/10.1039/d6su00045b.

Acknowledgements

The authors gratefully acknowledge the Cargill Company for kindly providing Pripol™ 1009, used in the development of the resin systems. Additionally, the authors would like to thank the Fraunhofer Center for Chemical-Biotechnological Processes CBP for kindly donating the lignin used in this work. The authors also thank the entire Division of Coating Technology at KTH Royal Institute of Technology for their technical support and valuable discussions. Financial support for the research-stay abroad was provided by the Karlsruhe House of Young Scientists (KHYS).

References

1 A. R. Kakroodi, M. Sain, 10 - Lignin-Reinforced Rubber Composites. in *Lignin in Polymer Composites*, O. Faruk and M. Sain, ed. William Andrew Publishing, 2016, pp. 195–206, DOI: 10.1016/B978-0-323-35565-0.00010-2.

2 J. Carlos Del Río, J. Rencoret, A. Gutiérrez, H. Kim and J. Ralph, Hydroxystilbenes Are Monomers in Palm Fruit Endocarp Lignins, *Plant Physiol.*, 2017, **174**(4), 2072–2082, DOI: 10.1104/pp.17.00362.

3 J. Rencoret, D. Neiva, G. Marques, A. Gutiérrez, H. Kim, J. Gominho, H. Pereira, J. Ralph and J. C. Del Río, Hydroxystilbene Glucosides Are Incorporated into Norway Spruce Bark Lignin, *Plant Physiol.*, 2019, **180**(3), 1310–1321, DOI: 10.1104/pp.19.00344.

4 J. C. Del Río, J. Rencoret, A. Gutiérrez, T. Elder, H. Kim and J. Ralph, Lignin Monomers from beyond the Canonical Monolignol Biosynthetic Pathway: Another Brick in the Wall, *ACS Sustainable Chem. Eng.*, 2020, **8**(13), 4997–5012, DOI: 10.1021/acssuschemeng.0c01109.

5 A. Beaucamp, M. Muddasar, I. S. Amiinu, M. Moraes Leite, M. Culebras, K. Latha, M. C. Gutiérrez, D. Rodriguez-Padron, F. Del Monte, T. Kennedy, K. M. Ryan, R. Luque, M.-M. Titirici and M. N. Collins, Lignin for Energy Applications – State of the Art, Life Cycle, Technoeconomic Analysis and Future Trends, *Green Chem.*, 2022, **24**(21), 8193–8226, DOI: 10.1039/D2GC02724K.

6 Organosolv Lignin Market Summary. *Reports and Data*. https://www.reportsanddata.com/report-detail/organosolv-lignin-market (accessed 2026-01-22).

7 M. Melikoglu, Organosolv Lignin: A Comprehensive Review of Pretreatment Advancements and Biorefinery Integration, *Next Mater.*, 2025, **9**, 101136, DOI: 10.1016/j.nxmate.2025.101136.

8 A. Kumar, Anushree, J. Kumar and T. Bhaskar, Utilization of Lignin: A Sustainable and Eco-Friendly Approach, *J. Energy Inst.*, 2020, **93**(1), 235–271, DOI: 10.1016/j.joei.2019.03.005.

9 N. Zhou, W. P. D. W. Thilakarathna, Q. S. He and H. P. V. Rupasinghe, A Review: Depolymerization of Lignin to Generate High-Value Bio-Products: Opportunities, Challenges, and Prospects, *Front. Energy Res.*, 2022, **9**, 758744, DOI: 10.3389/fenrg.2021.758744.

10 A. Creteanu, C. N. Lungu and M. Lungu, Lignin: An Adaptable Biodegradable Polymer Used in Different Formulation Processes, *Pharmaceuticals*, 2024, **17**(10), 1406, DOI: 10.3390/ph17101406.

11 F. Brienza, D. Cannella, D. Montesdeoca, I. Cybulska and D. P. Debecker, A Guide to Lignin Valorization in Biorefineries: Traditional, Recent, and Forthcoming Approaches to Convert Raw Lignocellulose into Valuable Materials and Chemicals, *RSC Sustain.*, 2024, **2**(1), 37–90, DOI: 10.1039/D3SU00140G.

12 M. B. Figueirêdo, I. Hita, P. J. Deuss, R. H. Venderbosch and H. J. Heeres, Pyrolytic Lignin: A Promising Biorefinery Feedstock for the Production of Fuels and Valuable Chemicals, *Green Chem.*, 2022, **24**(12), 4680–4702, DOI: 10.1039/D2GC00302C.

13 P. S. Jiju, A. K. Patel, N. S. Shruthy, S. Shalu, C.-D. Dong and R. R. Singhania, Sustainability through Lignin Valorization: Recent Innovations and Applications Driving Industrial Transformation, *Bioresour. Bioprocess.*, 2025, **12**(1), 88, DOI: 10.1186/s40643-025-00929-x.

14 C. Libretti, L. Santos Correa and M. A. R. Meier, From Waste to Resource: Advancements in Sustainable Lignin Modification, *Green Chem.*, 2024, **26**(8), 4358–4386, DOI: 10.1039/D4GC00745J.

15 M. Fazeli, S. Mukherjee, H. Baniasadi, R. Abidnejad, M. Mujtaba, J. Lipponen, J. Seppälä and O. J. Rojas, Lignin beyond the *Status Quo* : Recent and Emerging Composite Applications, *Green Chem.*, 2024, **26**(2), 593–630, DOI: 10.1039/D3GC03154C.

16 E. Bellinetto, N. Fumagalli, M. Astorri, S. Turri and G. Griffini, Elucidating the Role of Lignin Type and Functionality in the Development of High-Performance Biobased Phenolic Thermoset Resins, *ACS Appl. Polym. Mater.*, 2024, **6**(2), 1191–1203, DOI: 10.1021/acsapm.3c02136.

17 Y.-Y. Wang, C. E. Wyman, C. M. Cai and A. J. Ragauskas, Lignin-Based Polyurethanes from Unmodified Kraft Lignin Fractionated by Sequential Precipitation, *ACS Appl. Polym. Mater.*, 2019, **1**(7), 1672–1679, DOI: 10.1021/acsapm.9b00228.

18 M. Arefmanesh, S. Nikafshar, E. R. Master and M. Nejad, From Acetone Fractionation to Lignin-Based Phenolic and Polyurethane Resins, *Ind. Crops Prod.*, 2022, **178**, 114604, DOI: 10.1016/j.indcrop.2022.114604.

19 F. C. Destaso, C. Libretti, C. Le Coz, E. Grau, H. Cramail and M. A. R. Meier, Optimized Synthesis of a High Oleic Sunflower Oil Derived Polyamine and Its Lignin-Based NIPUs, *Green Chem.*, 2025, **27**(5), 1440–1450, DOI: 10.1039/D4GC05645K.

20 A. Salanti, L. Zoia, M. Mauri and M. Orlandi, Utilization of Cyclocarbonated Lignin as a Bio-Based Cross-Linker for the Preparation of Poly(Hydroxy Urethane)s, *RSC Adv.*, 2017, **7**(40), 25054–25065, DOI: 10.1039/C7RA03416D.

21 J. Sternberg and S. Pilla, Materials for the Biorefinery: High Bio-Content, Shape Memory Kraft Lignin-Derived Non-Isocyanate Polyurethane Foams Using a Non-Toxic Protocol, *Green Chem.*, 2020, **22**(20), 6922–6935, DOI: 10.1039/D0GC01659D.

22 S.-L. Zou, L.-P. Xiao, X.-Y. Li, W.-Z. Yin and R.-C. Sun, Lignin-Based Composites with Enhanced Mechanical Properties by Acetone Fractionation and Epoxidation Modification, *iScience*, 2023, **26**(3), 106187, DOI: 10.1016/j.isci.2023.106187.

23 L. C. Over, E. Grau, S. Grelier, M. A. R. Meier and H. Cramail, Synthesis and Characterization of Epoxy Thermosetting Polymers from Glycidylated Organosolv Lignin and Bisphenol A, *Macromol. Chem. Phys.*, 2017, **218**(4), 1600411, DOI: 10.1002/macp.201600411.

24 A. Shundo, S. Yamamoto and K. Tanaka, Network Formation and Physical Properties of Epoxy Resins for Future Practical Applications, *JACS Au*, 2022, **2**(7), 1522–1542, DOI: 10.1021/jacsau.2c00120.

25 C. Yang, F. Topuz, S.-H. Park and G. Szekely, Biobased Thin-Film Composite Membranes Comprising Priamine–Genipin Selective Layer on Nanofibrous Biodegradable Polylactic Acid Support for Oil and Solvent-Resistant Nanofiltration, *Green Chem.*, 2022, **24**(13), 5291–5303, DOI: 10.1039/D2GC01476A.

26 M. Z. Lisiecka, Biological Effects of Epoxy Resins on the Human Body: Toxicity and Allergic Reactions, *Drug Chem. Toxicol.*, 2025, 1–11, DOI: 10.1080/01480545.2025.2557405.

27 J. Park and S. Lee, Biodegradable Epoxy Thermosets Prepared by Mixing Diglycidyl Ether of Bisphenol A and Epoxidized Soybean Oil and Their Electrical and Mechanical Properties, *J. Appl. Polym. Sci.*, 2025, **142**(15), e56739, DOI: 10.1002/app.56739.

28 X. Yang, J. Li, Y. Wang, L. Tan, L. Han, J. Lu, M. Li, D. Fang, X. Huang, Y. Xu and C. Zhang, Synthesis and Characterization of Fully Biobased Epoxy Elastomers Prepared from Different Plant Oils, *ACS Sustainable Chem. Eng.*, 2023, **11**(38), 13950–13961, DOI: 10.1021/acssuschemeng.3c02634.

29 S. Caillol, Cardanol: A Promising Building Block for Biobased Polymers and Additives, *Curr. Opin. Green Sustainable Chem.*, 2018, **14**, 26–32, DOI: 10.1016/j.cogsc.2018.05.002.

30 X. Zhou, Z. Yu, Y. Fang, H. Hu, S. Cheng, Z. Tang and Y. Liu, High-Performance Fully Bio-Based Dynamic Covalent Supramolecular Epoxy Resin: Synthesis and Properties, *Green Chem.*, 2025, **27**(12), 3248–3260, DOI: 10.1039/D4GC06425A.

31 H. Nabipour, X. Wang, L. Song and Y. Hu, A High Performance Fully Bio-Based Epoxy Thermoset from a Syringaldehyde-Derived Epoxy Monomer Cured by Furan-Derived Amine, *Green Chem.*, 2021, **23**(1), 501–510, DOI: 10.1039/D0GC03451G.

32 Z. Song, L. Liu, P. Zhang, K. Xue, Z. Hua, T. You, Y. Wu, H. Cui, Z. Hu and Y. Huang, Fully Bio-Based Acetal Diepoxy Monomer with High Modulus, Good Thermal Stability and Readily Degradability, *Polym. Chem.*, 2024, **15**(47), 4824–4834, DOI: 10.1039/D4PY01038H.

33 Epichlorohydrin in Drinking-Water, Background Document for Development of WHO Guidelines for Drinking-Water Quality, 2004. https://cdn.who.int/media/docs/default-source/wash-documents/wash-chemicals/epichlorohydrin-bd.pdf?sfvrsn=4dd62bab_4 (accessed 2025-09-30).

34 S. Ohshima, T. Shibata, N. Sasaki, H. Okuda, H. Nishizawa, M. Ohsawa, M. Matsumoto and E. Nakayama, Subacute toxicity of an amine-curing agent for epoxy resin, *Sangyo Igaku*, 1984, **26**(3), 197–204.

35 M. Z. Lisiecka, Biological Effects of Epoxy Resins on the Human Body: Toxicity and Allergic Reactions, *Drug Chem. Toxicol.*, 2025, 1–11, DOI: 10.1080/01480545.2025.2557405.

36 X. Shao, P. Zhao, Z. Tian, N. Zhang, H. Wang, X. Li, X. Cui, X. Hou and T. Deng, A Novel Bio-Based Anhydride Curing Agent for the Synthesis of High-Performance Epoxy Resin, *Polym. Degrad. Stab.*, 2024, **229**, 110979, DOI: 10.1016/j.polymdegradstab.2024.110979.

37 F. Jaillet, M. Desroches, R. Auvergne, B. Boutevin and S. Caillol, New Biobased Carboxylic Acid Hardeners for Epoxy Resins, *Eur. J. Lipid Sci. Technol.*, 2013, **115**(6), 698–708, DOI: 10.1002/ejlt.201200363.

38 F. Andriani, M. Karlsson, T. Elder and M. Lawoko, Lignin Carboxymethylation: Probing Fundamental Insights into Structure–Reactivity Relationships, *ACS Sustainable Chem. Eng.*, 2024, **12**(4), 1705–1713, DOI: 10.1021/acssuschemeng.3c07385.

39 F. Andriani and M. Lawoko, Oxidative Carboxylation of Lignin: Exploring Reactivity of Different Lignin Types, *Biomacromolecules*, 2024, **25**(7), 4246–4254, DOI: 10.1021/acs.biomac.4c00326.

40 X. Zhen, X. Cui, A. A. N. M. Al-Haimi, X. Wang, H. Liang, Z. Xu and Z. Wang, Fully Bio-Based Epoxy Resins from Lignin and Epoxidized Soybean Oil: Rigid-Flexible, Tunable Properties and High Lignin Content, *Int. J. Biol. Macromol.*, 2024, **254**, 127760, DOI: 10.1016/j.ijbiomac.2023.127760.

41 S. Zhou, K. Huang, X. Xu, B. Wang, W. Zhang, Y. Su, K. Hu, C. Zhang, J. Zhu, G. Weng and S. Ma, Rigid-and-Flexible, Degradable, Fully Biobased Thermosets from Lignin and Soybean Oil: Synthesis and Properties, *ACS Sustainable Chem. Eng.*, 2023, **11**(8), 3466–3473, DOI: 10.1021/acssuschemeng.2c06990.

42 G. Resende, G. D. Azevedo, F. Souto and V. Calado, Chemical Modification of Softwood Kraft Lignin with Succinic Acid, *ACS Omega*, 2024, **9**(52), 50945–50956, DOI: 10.1021/acsomega.4c03127.

43 S. Hirose, T. Hatakeyama and H. Hatakeyama, Glass Transition and Thermal Decomposition of Epoxy Resins from the Carboxylic Acid System Consisting of Ester-Carboxylic Acid Derivatives of Alcoholysis Lignin and Ethylene Glycol with Various Dicarboxylic Acids, *Thermochim. Acta*, 2005, **431**(1–2), 76–80, DOI: 10.1016/j.tca.2005.01.043.

44 S. Hirose, T. Hatakeyama and H. Hatakeyama, Synthesis and Thermal Properties of Epoxy Resins from Ester-carboxylic Acid Derivative of Alcoholysis Lignin, *Macromol. Symp.*, 2003, **197**(1), 157–170, DOI: 10.1002/masy.200350715.

45 C. Scarica, R. Suriano, M. Levi, S. Turri and G. Griffini, Lignin Functionalized with Succinic Anhydride as Building Block for Biobased Thermosetting Polyester Coatings, *ACS Sustainable Chem. Eng.*, 2018, **6**(3), 3392–3401, DOI: 10.1021/acssuschemeng.7b03583.

46 E. Subbotina, P. Olsén, M. Lawoko and L. A. Berglund, Maleated Technical Lignin Thermosets and Biocomposites Designed for Degradation, *ACS Sustainable Chem. Eng.*, 2024, **12**(9), 3632–3642, DOI: 10.1021/acssuschemeng.3c06741.

47 F. Haitz, S. Radloff, S. Rupp, M. Fröhling, T. Hirth and S. Zibek, Chemo-Enzymatic Epoxidation of Lallemantia IbericaSeed Oil: Process Development and Economic-Ecological Evaluation, *Appl. Biochem. Biotechnol.*, 2018, **185**(1), 13–33, DOI: 10.1007/s12010-017-2630-1.

48 B. Hashim, W. U. Khan, D. Hantoko, G. A. Nasser, M. A. Sanhoob, A. I. Bakare, N. S. Govender, S. A. Ali and M. M. Hossain, *N* -Butane Oxidation to Maleic Anhydride: Reaction Mechanism and Kinetics Over VPO Catalyst, *Ind. Eng. Chem. Res.*, 2024, **63**(14), 5987–6002, DOI: 10.1021/acs.iecr.3c04371.

49 A. Kanzow, B. Hartwig, P. Buschmann, K. G. Lengsfeld, C. M. Höhne, J. S. Hoke, F. Knüppe, F. Köster, J. K. Van Spronsen, J.-U. Grabow, D. McNaughton and D. A. Obenchain, Tautomer Identification Troubles: The Molecular Structure of Itaconic and Citraconic Anhydride Revealed by Rotational Spectroscopy, *Phys. Chem. Chem. Phys.*, 2025, **27**(18), 9491–9503, DOI: 10.1039/D5CP00389J.

50 Maleic Anhydride; MSDS No. 63200 [Online]; Sigma-Aldrich Chemie GmbH, Taufkirchen, DE. https://www.sigmaaldrich.com/DE/en/sds/sial/63200?userType=undefined.

51 Itaconic Anhydride; MSDS No. 259926 [Online]; Sigma-Aldrich Chemie GmbH, Taufkirchen, DE. https://www.sigmaaldrich.com/DE/en/sds/aldrich/259926?userType=anonymous.

52 T. Robert and S. Friebel, Itaconic Acid – a Versatile Building Block for Renewable Polyesters with Enhanced Functionality, *Green Chem.*, 2016, **18**(10), 2922–2934, DOI: 10.1039/C6GC00605A.

53 Th. Willke and K.-D. Vorlop, Biotechnological Production of Itaconic Acid, *Appl. Microbiol. Biotechnol.*, 2001, **56**(3–4), 289–295, DOI: 10.1007/s002530100685.

54 U. Biermann, U. T. Bornscheuer, I. Feussner, M. A. R. Meier and J. O. Metzger, Fatty Acids and Their Derivatives as Renewable Platform Molecules for the Chemical Industry, *Angew. Chem., Int. Ed.*, 2021, **60**(37), 20144–20165, DOI: 10.1002/anie.202100778.

55 E. C. Leonard, Polymerization-dimer Acids, *J. Am. Oil Chem. Soc.*, 1979, **56**(11 Part 2), 782A–785A, DOI: 10.1007/BF02667445.

56 R. K. Henderson, C. Jiménez-González, D. J. C. Constable, S. R. Alston, G. G. A. Inglis, G. Fisher, J. Sherwood, S. P. Binks and A. D. Curzons, Expanding GSK's Solvent Selection Guide – Embedding Sustainability into Solvent Selection Starting at Medicinal Chemistry, *Green Chem.*, 2011, **13**(4), 854, DOI: 10.1039/c0gc00918k.

57 E. Fritz-Langhals, Unique Superbase TBD (1,5,7-Triazabicyclo[4.4.0]Dec-5-Ene): From Catalytic Activity and One-Pot Synthesis to Broader Application in Industrial Chemistry, *Org. Process Res. Dev.*, 2022, **26**(11), 3015–3023, DOI: 10.1021/acs.oprd.2c00248.

58 I. Flores, J. Demarteau, A. J. Müller, A. Etxeberria, L. Irusta, F. Bergman, C. Koning and H. Sardon, Screening of Different Organocatalysts for the Sustainable Synthesis of PET, *Eur. Polym. J.*, 2018, **104**, 170–176, DOI: 10.1016/j.eurpolymj.2018.04.040.

59 1,1,3,3-Tetramethylguanidine; MSDS No. 241768 [Online]; Sigma-Aldrich Chemie GmbH, Taufkirchen, DE, 2025. https://www.sigmaaldrich.com/DE/en/sds/aldrich/241768?userType=anonymous (accessed 2025-02-19).

60 1,8-Diazabicyclo[5.4.0]Undec-7-Ene; MSDS No. 139009 [Online]; Sigma-Aldrich Chemie GmbH, Taufkirchen, DE, 2023. https://www.sigmaaldrich.com/DE/en/sds/aldrich/139009?userType=anonymous (accessed 2025-02-19).

61 E. Subbotina, P. Olsén, M. Lawoko and L. A. Berglund, Maleated Technical Lignin Thermosets and Biocomposites Designed for Degradation, *ACS Sustainable Chem. Eng.*, 2024, **12**(9), 3632–3642, DOI: 10.1021/acssuschemeng.3c06741.

62 W. G. Barb, Interconversions of Itaconic and Citraconic Anhydride in Amine Solutions, *J. Chem. Soc.*, 1955, 1647–1651, DOI: 10.1039/jr9550001647.

63 M. C. Galanti and A. V. Galanti, Kinetic Study of the Isomerization of Itaconic Anhydride to Citraconic Anhydride, *J. Org. Chem.*, 1981, **47**(8), 1572–1574.
64 K. F. Long, H. Wang, T. T. Dimos and C. N. Bowman, Effects of Thiol Substitution on the Kinetics and Efficiency of Thiol-Michael Reactions and Polymerizations, *Macromolecules*, 2021, **54**(7), 3093–3100, DOI: 10.1021/acs.macromol.0c02677.
65 R. Connor and Wm. R. McClellan, The Michael Condensation. V*. The Influence of the Experimental Conditions and the Structure of the Acceptor Upon the Condensation, *J. Org. Chem.*, 1939, **3**(6), 570–577, DOI: 10.1021/jo01223a005.
66 H. Silau, A. G. Garcia, J. M. Woodley, K. Dam-Johansen and A. E. Daugaard, Bio-Based Epoxy Binders from Lignin Derivatized with Epoxidized Rapeseed Fatty Acids in Bimodal Coating Systems, *ACS Appl. Polym. Mater.*, 2022, **4**(1), 444–451, DOI: 10.1021/acsapm.1c01351.
67 S. Laurichesse, C. Huillet and L. Avérous, Original Polyols Based on Organosolv Lignin and Fatty Acids: New Bio-Based Building Blocks for Segmented Polyurethane Synthesis, *Green Chem.*, 2014, **16**(8), 3958–3970, DOI: 10.1039/C4GC00596A.
68 F. Mustata and N. Tudorachi, Curing Kinetics and Thermal Characterization of Epoxy Resin Cured with Amidodicarboxylic Acids, *Appl. Therm. Eng.*, 2017, **125**, 285–296, DOI: 10.1016/j.applthermaleng.2017.07.037.
69 F. Rothenhäusler, M. Kettenbach and H. Ruckdaeschel, Influence of the Stoichiometric Ratio on the Curing Kinetics and Mechanical Properties of Epoxy Resin Cured with a Rosin-Based Anhydride, *Macromol. Mater. Eng.*, 2023, **308**(11), 2300122, DOI: 10.1002/mame.202300122.
70 F. Jing, R. Zhao, C. Li, Z. Xi, Q. Wang and H. Xie, Influence of the Epoxy/Acid Stoichiometry on the Cure Behavior and Mechanical Properties of Epoxy Vitrimers, *Molecules*, 2022, **27**(19), 6335, DOI: 10.3390/molecules27196335.
71 G. Couture, L. Granado, F. Fanget, B. Boutevin and S. Caillol, Limonene-Based Epoxy: Anhydride Thermoset Reaction Study, *Molecules*, 2018, **23**(11), 2739, DOI: 10.3390/molecules23112739.
72 K. Huang, P. Zhang, J. Zhang, S. Li, M. Li, J. Xia and Y. Zhou, Preparation of Biobased Epoxies Using Tung Oil Fatty Acid-Derived C21 Diacid and C22 Triacid and Study of Epoxy Properties, *Green Chem.*, 2013, **15**(9), 2466, DOI: 10.1039/c3gc40622a.
73 C. Ding, P. S. Shuttleworth, S. Makin, J. H. Clark and A. S. Matharu, New Insights into the Curing of Epoxidized Linseed Oil with Dicarboxylic Acids, *Green Chem.*, 2015, **17**(7), 4000–4008, DOI: 10.1039/C5GC00912J.
74 A. Duval, W. Benali and L. Avérous, Turning Lignin into a Recyclable Bioresource: Transesterification Vitrimers from Lignins Modified with Ethylene Carbonate, *Green Chem.*, 2024, **26**(14), 8414–8427, DOI: 10.1039/D4GC00567H.
75 A. Duval, W. Benali and L. Avérous, Exploiting Lignin Structure and Reactivity to Design Vitrimers with Controlled Ratio of Dynamic to Non-Dynamic Bonds, *ChemSusChem*, 2025, **18**(3), e202401480, DOI: 10.1002/cssc.202401480.